

Kinetics and steady state of polar flock with birth and death

Pratikshya Jena^{1*} and Shradha Mishra^{1†}
Indian Institute of Technology (BHU)

(Dated: December 16, 2022)

We study a collection of polar self-propelled particles or polar flock on a two dimensional substrate with birth and death. Most of the previous studies of polar flock with birth and death have assumed the compressible flock, such that the local density of flock is completely ignored. Effect of birth and death of particles on the flock with moderate density is focus of our study. System is modeled using coarse-grained hydrodynamic equations of motion for local density and velocity of the flock and solved using numerical integration of the nonlinear coupled partial differential equations of motion and linearised hydrodynamics about the broken symmetry state. We studied the ordering kinetics as well as the steady state properties of the immortal flock and flock with finite birth and death rate. The ordering kinetics of the velocity field remains unaffected whereas the density field shows a crossover from asymptotic growth exponent 5/6 for the immortal flock to diffusive limit 1/3 for large birth and death rates. In the steady state, the presence of birth and death rate leads to the suppression of speed of sound wave and density fluctuations in the system.

I. INTRODUCTION

Active matter [1–6] is a novel class of nonequilibrium systems which consist of interacting units that consume energy individually and generate motion and mechanical stress collectively. Each individual unit contains an intrinsic asymmetry and have tendency to self-propelled along the direction of asymmetry. Such systems span a huge range of length scales, starting from very small scales of few microns sized molecular motors, bacterial colonies, cells, cytoskeleton filaments etc. to large scales of the order of few meters and kilometers such as bird flock, human crowd, animal herd etc. [7–13]. The collection of such particles show interesting features such as pattern formation [14], nonequilibrium disorder to order transitions [15–20], anomalous fluctuations [21] etc., those are not present in corresponding analogous equilibrium systems.

Flocking [3] or collective and coherent motion of large number of organisms is the most interesting and ubiquitous phenomenon in many biological systems. Unlike the corresponding equilibrium system [22], flock shows a true long ranged, long time behavior in two dimensions. The appearance of dense ordered clusters of particles, propagating sound modes and the giant number fluctuation are observed [23] in flock in the steady state.

Most of the previous studies of polar flock focused on the immortal flock, where number of particles remain constant [17, 24–26]. In a recent study [27], the author studied a system of polar flock without number conservation and showed that the system behaves differently from the immortal flock i.e, the longitudinal velocity fluctuations in the direction of flock motion replace the sound modes of number conserving flock. The study of [27] focused on the high density limit of polar flock with birth and death, such that the density field is completely ignored. The properties of immortal flock with finite density is

not explored, and it is the focus of our study.

In this letter, we study the polar flock without number conservation (Malthusian flock) [28]. We model the collection of polar self-propelled particles with birth and death. We write the coarse-grained hydrodynamic equations of motion for local density and velocity and study it using numerical solution of nonlinear coupled partial differential equations of motion and linearised hydrodynamics about the broken symmetry state.

Starting from random homogeneous ordered state of density and velocity, we study the ordering kinetics of both the fields and find that the ordering of velocity field remains unaffected due to birth and death, whereas the density field shows a strong dependence on the birth and death rate. Density shows an asymptotic growth law of 5/6 [27] for immortal flock and low birth and death rate. For large birth and death rate the approach to asymptotic growth is faster and towards the diffusive growth law 1/3 [29]. In the steady state, the presence of birth and death rate suppresses the speed of traversing sound mode and density fluctuations in the system.

II. MODEL

We model a collection of polar self-propelled particles with birth and death. We approach the problem using coarse-grained hydrodynamic equations of motion for two slow variables, viz (i) local density $\rho(\mathbf{r}, t)$ and (ii) velocity $\mathbf{v}(\mathbf{r}, t)$ of particles at position \mathbf{r} and at time t . The hydrodynamic equation for the density $\rho(\mathbf{r}, t)$ is:

$$\partial_t \rho + v_0 \nabla \cdot (\mathbf{v} \rho) = D_\rho \nabla^2 \rho + g(\rho) \quad (1)$$

and for the local velocity $\mathbf{v}(\mathbf{r}, t)$ is:

$$\partial_t \mathbf{v} + \lambda_1 (\mathbf{v} \cdot \nabla) \mathbf{v} + \lambda_2 (\nabla \cdot \mathbf{v}) \mathbf{v} = \alpha(\rho) \mathbf{v} - \beta |\mathbf{v}|^2 \mathbf{v} - \sigma_1 \nabla \rho + D_T \nabla^2 \mathbf{v} + \mathbf{f} \quad (2)$$

The density equation is continuity equation with addition to birth and death. The term on the left hand side

* pratikshya.jena.rs.phy20@iitbhu.ac.in

† smishra.phy@iitbhu.ac.in

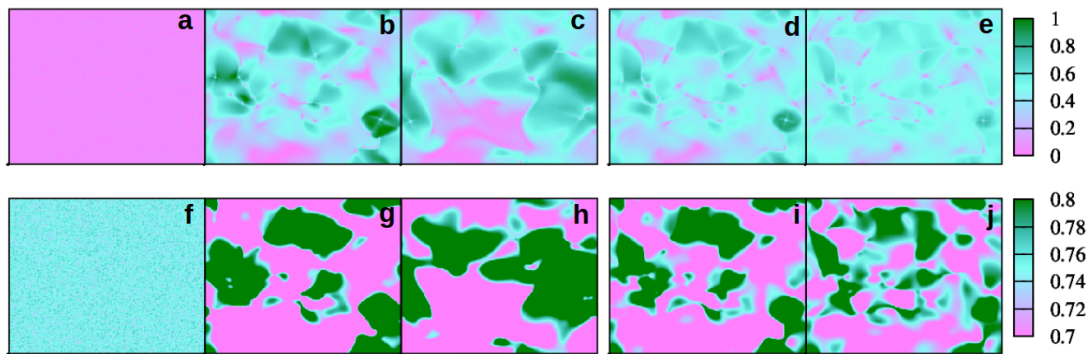


FIG. 1: (color online) Real space snapshots of local velocity $v(\mathbf{r}, t)$ (upper panel) ($a - c$) and density $\rho(\mathbf{r}, t)$ (lower panel) ($f - h$) for the IF and at times $t = 0, 900$ and 200 respectively. ($d - e$) and ($i - j$) are the snapshots for local velocity and density respectively at fixed time $t = 900$ and for different $\lambda = 0.05, 0.1$.

is the current due to self-propulsion. The first term on the right side is the diffusion current and the last term is an additional birth and death term of the form $g(\rho) = \lambda\rho(1 - \frac{\rho}{\rho_0})$. The parameter λ controls the rate of birth and death. For $\lambda = 0$, the model reduces to the immortal flock (IF) [25] and for finite λ we have flock with birth and death (MF) [30, 31]. Here, ρ_0 is constant that controls the mean density. The velocity Eq.2 is the same as introduced by Toner and Tu for the immortal flock [25]. In Eq.2, the right hand side, the terms, $\alpha(\rho)\mathbf{v}$, $\beta|\mathbf{v}|^2\mathbf{v}$ and $D_T\nabla^2\mathbf{v}$ arise in analogy with the time dependent Ginzburg-Landau equation (TDGL) [32] which is responsible for ordering towards the broken symmetry phase. $\lambda_1(\mathbf{v} \cdot \nabla)\mathbf{v}$, $\sigma_1\nabla\rho$ terms are analogous to the convection and pressure due to gradient in density respectively and similar to the terms present in Navier-Stoke's equation for fluid dynamics. $\lambda_2(\nabla \cdot \mathbf{v})\mathbf{v}$ is another convective non linearity appears due to absence of Galilean invariance in the system. The last term in Eq.2 $\mathbf{f}(\mathbf{r}, t) = (f_1, f_2)$ is a random driving force representing noise and it is Gaussian with white-noise correlation and strength Δ ;

$$\langle f_i(\mathbf{r}, t)f_j(\mathbf{r}', t') \rangle = \Delta\delta_{ij}\delta(\mathbf{r} - \mathbf{r}')\delta(t - t') \quad (3)$$

Numerical integration of Eq.1 and 2 is performed with homogeneous initial density (with mean $\rho_0 = 0.75$) and random velocity in a box of size $K \times K$ with periodic boundary condition in the both directions. The integration is performed using Euler's scheme [33] with $\Delta x = 1.0$ and $\Delta t = 0.1$. The other parameters of the system are fixed to $\beta = 1.0$, $\lambda_1 = 0.5$, $\lambda_2 = 1.0$, $\alpha(\rho) = (1 - \rho/\rho_c)$ ($\rho_c = 0.5$), $D_\rho = 1.0$, $\sigma_1 = v_0/\rho_0$, $D_T = 1.0$, $v_0 = 0.5$ and varied the birth and death rate λ from 0 to 1.0. We checked that our numerical integration is stable for the above choice of parameters. The simulation is carried out by varying the system size i.e $K = 256$ to 2048 . Starting with random homogeneous state, system is quenched to the above parameters such that steady state is an ordered state. We studied the ordering kinetics of the velocity and the density

field and properties of the steady state for different birth and death rate λ . Steady state results are obtained for $K = 256$ to 1000 for time $t = 2 \times 10^5$ whereas coarsening studies are performed on relatively large system size $K = 2048$ with final time $t = 7 \times 10^3$. For better statistical averaging results are averaged over 100 independent realisations.

III. RESULT

We first plot the time evolution of real space snapshots of the system, initiated with random homogeneous state. Fig.1 show the time evolution of local velocity $v(\mathbf{r}, t) = |\mathbf{v}|$ (upper panel) and magnitude of local density $\rho(\mathbf{r}, t)$ (lower panel). Fig.1($a - c$; $f - h$) shows the plot for the immortal flock at three different times $t = 0, 900$ and 2000 and Fig 1($d - e$; $i - j$) is for the fixed time $t = 900$ and different $\lambda = 0.05$ and 0.1 respectively. As observed from the Fig.1($a - c$), the velocity field shows that system evolves towards the ordered state with the growing domains of ordered region with large magnitude of local v . Also the domains of high density region grows with time as shown in Fig.1($f - h$). The growing domains of ordered velocity and high density is also affected by increasing λ as shown in Fig. 1($d - e$; $i - j$) for fixed time and varying λ . The growth is more affected for density Fig. 1($i - j$) in comparison to velocity field Fig. 1($d - e$). The characteristics of the growing domains is measured by calculating the two-point velocity and density correlation functions $C_v(r, t) = \langle \mathbf{v}(\mathbf{r}_0, t) \cdot \mathbf{v}(\mathbf{r}_0 + \mathbf{r}, t) \rangle$ and $C_\rho(r, t) = \langle \delta\rho(\mathbf{r}_0, t)\delta\rho(\mathbf{r}_0 + \mathbf{r}, t) \rangle$ respectively. Here, $\delta\rho$ represents the fluctuation in density from the mean ρ_0 and the $\langle \dots \rangle$ means averaging over directions, reference points \mathbf{r}_0 and over 100 independent realisations. *Ordering kinetics*:- We define the size of the growing domain of by calculating the characteristics lengths $L_{v,\rho}(t)$ defined by the distance by which the the two-point correlation functions (as shown in Fig.1(a-b) (SM1)) decay to 0.1 of its value at $r = 0$. Fig.2(a-b) respectively shows the plot of the two characteristic lengths $L_{v,\rho}(t)$

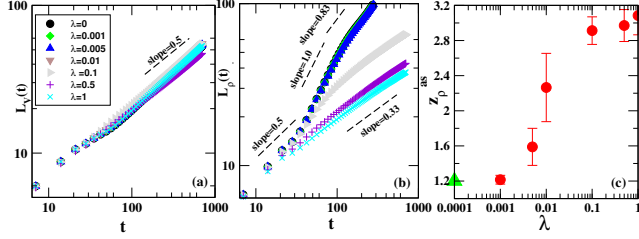


FIG. 2: (color online) (a,b) represent the log – log plot of characteristic lengths $L_{v,\rho}(t)$ vs. time t for velocity and density field respectively for different λ values. The dashed lines have their respective slopes as shown on top of them. (c) plot of z_ρ^{as} vs. λ . The solid \triangle on the y -axis is value 1.2.

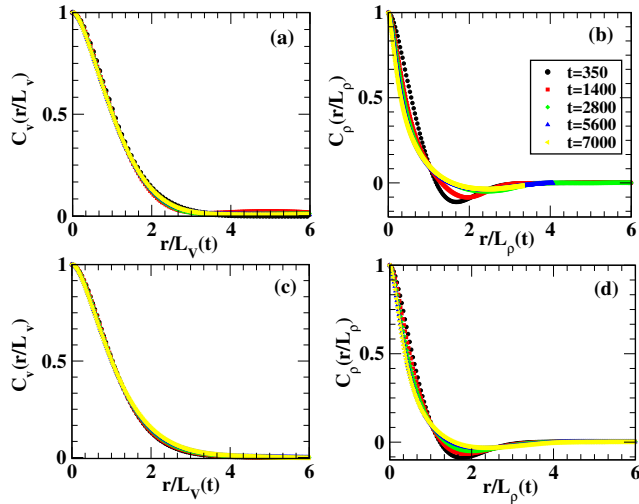


FIG. 3: (color online) The plot of scaled two-point correlation functions $C_{v,\rho}(r/L_{v,\rho}(t))$ vs. scaled distance $r/L_{v,\rho}(t)$ for velocity and density fields. (a – b) is for the IF ($\lambda = 0$) and (c – d) is for the MF with $\lambda = 0.01$. Different colors are for different times as shown in the legend.

vs. time t for different λ 's from 0 to 1. We find that the growth of $L_v(t)$ remains almost independent of λ . For all the cases the asymptotic growth law is 0.5 as shown by the dashed line. Hence the kinetics of velocity remains unaffected due to the birth and death parameter λ and remains the same as for the usual non-conserved growth kinetics of *Model A* [34, 35]. As shown in Fig.2(b) the growth of $L_\rho(t)$ shows strong dependence on the parameter λ . For immortal flock and weak birth and death $\lambda \leq 0.01$, the growth of $L_\rho(t)$ clearly shows three regimes. For very early time, the growth is mostly dominated by background non-conserved continuous velocity field and $L_\rho(t) \simeq t^{0.5}$, as we increase time, density starts to grow much faster and $L_\rho(t) \simeq t$. The fast growth is due to the hydrodynamic modes present in moving ordered flock [3, 17, 24]. Then at the late times $L_\rho(t)$ approaches to the asymptotic growth law $\simeq t^{5/6}$ predicted for the continuum theory of polar flock [25].

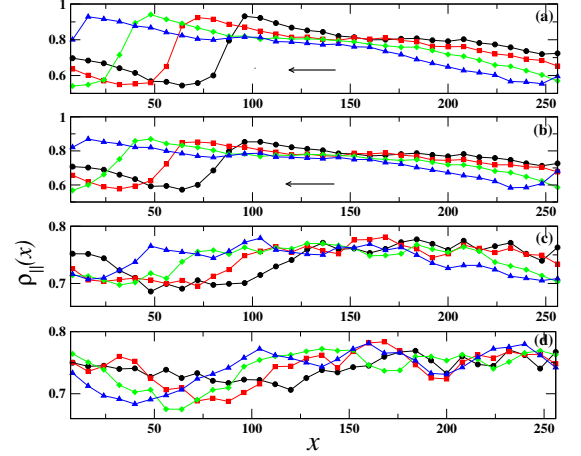


FIG. 4: (color online) (a – d), the plot of $\rho_{||}(x)$ vs. x for $\lambda = 0, 0.0005, 0.0008, 0.001$ respectively. Different colors/symbols \circ (black), \square (red), \diamond (green) and \triangle (blue) in each window represent the different times ($t_1 < t_2 < t_3 < t_4$) respectively in the steady state at the interval of $t = 400$. The arrows in (a – b) show the direction of moving flock.

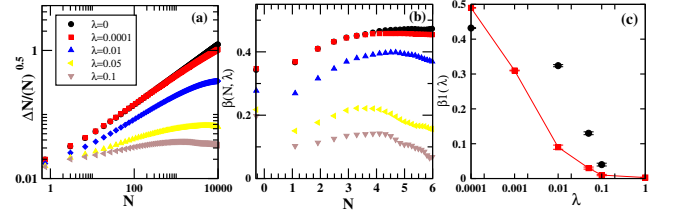


FIG. 5: (color online) (a) The log – log plot of $\frac{\Delta N}{\sqrt{N}}$ vs. N for different λ . (b) The plot of $\beta(N, \lambda)$ vs. N . (c) The plot of $\beta(\lambda)$ vs. λ . The black data are obtained from numerical simulation and data with line (red) obtained from Eq. 21 in VI by putting all the constants from the numerical simulation.

On increasing $\lambda > 0.01$, the approach to the asymptotic growth happens early and asymptotic growth exponent decreases with increasing λ and finally for large λ 's it approaches to the diffusive limit with $L_\rho(t) \sim t^{1/3}$ for the conserved growth kinetics [36]. In Fig.2(c) we show the plot of asymptotic growth exponent z_ρ^{as} vs. λ , where z_ρ^{as} is obtained from the late time power law dependence of $L_\rho(t) \simeq t^{1/z_\rho^{as}}$ in the main figure. We found that for very small $\lambda < 0.001$, $z_\rho^{as} \simeq 6/5$ and then it increases with increasing λ and saturate to the diffusion limit $\simeq 3$ for higher λ . Hence asymptotic growth of the density is driven by the conventional sound mode propagating in the direction parallel to the direction of flock; for the IF and flock with small birth and death rate, whereas it is purely diffusive for the MF.

We further characterise the scaling behaviour of two-point correlation functions. In Fig.3(a-b) we show the plot of scaled correlations for velocity and density $C_v(r/L_v(t))$ and $C_\rho(r/L_\rho(t))$ respectively for the IF,

$\lambda = 0.0$ and in Fig.3(c - d) for the $\lambda = 0.01$ and for different times. We find that for both the cases IF and $\lambda = 0.01$, the velocity field $C_v(r/L_v(t))$ shows the good scaling collapse, whereas density $C_\rho(r/L_\rho(t))$ does not. Non scaling of density field for immortal flock is also reported in previous studies [35], is due to the presence of more than one regime of growing domain as shown in $L_\rho(t)$ in Fig.2(b) [37].

Steady state:- Now we explore the effect of birth and death on the steady state properties of the system. One of the characteristics of immortal flock is the formation of ordered high density bands moving in the low density disordered background. These bands move as the sound wave travelling along the ordering direction of the flock [16, 17, 31, 37]. In SM2, we show the animations of local density in the steady state for different λ 's = 0, 0.0005, 0.0008, 0.001 for system of size $L = 256$. It can be observed that the density fluctuations as well as the speed of the moving bands decreases with increasing λ . To further quantify the motion of travelling density pattern for different λ , we define the one dimensional density profile $\rho_{\parallel}(x)$, by averaging the local density $\rho(\mathbf{r}, t)$ over the direction transverse to the propagating direction of the band i.e, $\rho_{\parallel}(x) = \frac{\sum_{j=1}^L \rho_{j,\perp}}{L}$; here, $\rho_{\perp,\parallel}$ is the density along the transverse and longitudinal direction of the global orientation direction of the flock respectively. x is chosen as the travelling direction (direction of ordering of the flock) of the bands. In the Fig.4 (a - d), we show the plot of $\rho_{\parallel}(x)$ for four different λ 's = 0, 0.0005, 0.0008 and 0.001 respectively. Different colors in each plot represents the $\rho_{\parallel}(x)$ at four different times at the interval of $t = 400$. We find that for $\lambda = 0$, the pattern of $\rho_{\parallel}(x)$ shifts towards the direction of propagating band (shown by the arrow). The shift is proportional to the speed of the bands. As we introduce λ , and on increasing it, the shift as well as the amplitude of fluctuation reduces and for $\lambda > 0.0005$, the band fades away and density approaches to the mean value $\rho_0 = 0.75$ at late times. We also calculated the sound speed using the linearised hydrodynamic equations of motion for the two fields (\mathbf{v} and ρ). The SM1, contains the details of the calculation. We find that sound speed very much depends on the birth and death rate and decreases with increasing λ as given in Eq.14 (VI). Also interestingly we find that the sound speed is purely non-dispersive for IF ($\lambda = 0$) and becomes dispersive for finite λ Eq.14 (VI) (although the dependence is quadratic in λ). In VI we show the plot of $\rho_{\parallel}(x)$ for three different system sizes $K = 175, 200, 256$ for $\lambda = 0.0005$. Clearly the speed of the band depends on K and increases on increasing K .

Further we also calculate the effect of λ on the number fluctuation ΔN of particle density and compared it with the density fluctuation calculated from the linearised approximation. The details of the linear calculation using coarse-grained hydrodynamic equations is given in VI. In Fig.5(a) we show the plot of $\frac{\Delta N}{\sqrt{N}}$ vs. N for different λ values. We expect the $\frac{\Delta N}{\sqrt{N}} \simeq N^\alpha$, where the exponent $\alpha > 0$ for density fluctuation larger than the correspond-

ing equilibrium systems [38]. We find that for $\lambda \leq 0.05$, density fluctuation is larger than the equilibrium and for higher $\lambda > 0.05$, it is suppressed. Further in Fig 5(b) we plot $\beta(N, \lambda)$ vs. N , where $\beta(N, \lambda)$ is obtained by $\beta(N, \lambda) = \frac{d \ln \frac{\Delta N}{\sqrt{N}}}{d \ln N}$. For small N , $\beta(N, \lambda)$ increases with N and for large N it approaches to value = 0.4, for $\lambda \leq 0.05$ and zero for large $\lambda > 0.05$. In Fig. 5(c) we show the plot of $\beta(\lambda)$ for different λ ; where $\beta(\lambda)$ is obtained from the large N limit of $\beta(N, \lambda)$ from the previous plot. The data (black) shows the calculation from the numerical results and red data (lines) is the prediction from the linearised hydrodynamics (VI Eq.21). We find that for small λ , linearised theory under predicts the behaviour of $\beta(\lambda)$, whereas for large λ it approaches to zero and numerical result matches with theoretical prediction.

IV. SUMMARY

In this letter, we have modeled the Malthusian flock with birth and death rate in two-dimensions using coarse-grained hydrodynamic equations of motion for local velocity and density. Unlike the previous study of [27] for high density, our study is focused on the finite density of particles, such that density field cannot be ignored. Starting from the random homogeneous state; the ordering kinetics of the system towards the ordered state is studied using numerical integration of the coupled non-linear partial differential equations of motion for the two fields. We find that the ordering kinetics of the velocity field remains unaffected due to birth and death rate, but density shows strong dependence. For IF and small birth and death rate the asymptotic growth law for density is 5/6 and shows a crossover to diffusive growth law of 1/3 for large birth and death rate. The approach to asymptotic growth becomes faster as we increase the birth and death rate. We also characterised the steady state properties of the flock using both numerical integration of full non-linear equations and linearised hydrodynamic about the ordered state and find that the presence of finite birth and death rate suppresses the speed of sound wave and large density fluctuations present in the immortal flock [27].

Our study shows the effect of birth and death rate on the ordering kinetics and steady state properties of polar self-propelled particles for the case when density fluctuations are taken in account. Hence it can be used to understand the effect of birth and death in various biophysical systems with moderate densities [39–43]. Our finding can be tested for similar experiments[44] in the laboratory.

V. ACKNOWLEDGMENTS

P.J. gratefully acknowledge the DST INSPIRE fellowship for funding this project. The support and the resources provided by PARAM Shivay Facility under the

National Supercomputing Mission, Government of India at the Indian Institute of Technology, Varanasi are gratefully acknowledged by all authors. S.M. thanks DST-SERB India, ECR/2017/000659 and CRG/2021/006945 for financial support. P.J. and S.M. also thank the Centre for Computing and Information Services at IIT (BHU), Varanasi.

VI. APPENDIX

A. Ordering kinetics

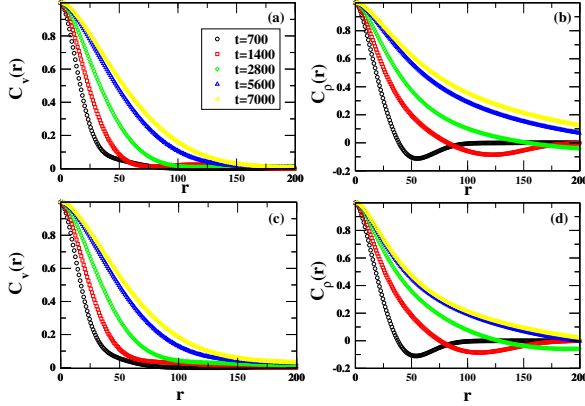


FIG. 6: (color online) The plot of two-point correlation functions $C_{v,\rho}(r)$ vs. distance r for velocity and density fields. (a – b) is for the IF ($\lambda = 0$) and (c – d) is for the MF with $\lambda = 0.01$. Different colors are for different times as shown in the legend.

B. Steady state

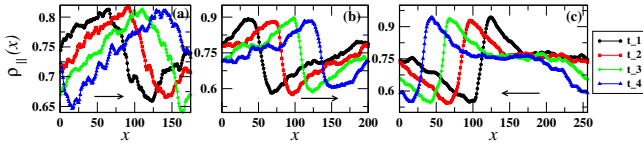


FIG. 7: (color online) The plot of $\rho_{\parallel}(x)$ vs. x for $\lambda = 0.0005$ for three different system sizes (a – c); $K = 175, 200$ and 256 respectively for four different times $t_1 < t_2 < t_3 < t_4$ in the steady state at the time interval of $t = 400$. The arrows in each figure represent the direction of moving flock.

C. Linearized approximation

In this section we focus on the linearised hydrodynamics of the system about the broken symmetry state. The steady state solution of Eq.1 and Eq.2 in the main text is a homogeneous ordered state with density $\rho = \rho_0$

and order parameter $\mathbf{v} = v_0 \hat{x}$, where $v_0 = \sqrt{\frac{\alpha}{\beta}}$ and $\alpha = \alpha_0(1 - \rho_0/\rho_c)$. Here we have chosen \hat{x} as the direction of broken symmetry. We add small fluctuations to the uniformly ordered velocity and homogeneous density, and write the velocity field as $\mathbf{v} = v_0 \hat{x} + \delta \mathbf{v}$. The fluctuation in \mathbf{v} , $\delta \mathbf{v} = (v_{\parallel} \hat{x}, v_{\perp} \hat{y})$, where \hat{y} is direction perpendicular to the ordering direction. Now we write the equation of motion for the fluctuation δv_{\parallel} to the linear order in small fluctuations ($\delta \rho, v_{\parallel}, v_{\perp}$)

$$\partial_t v_{\parallel} = -\sigma_1 \partial_{\parallel} \delta \rho - 2\alpha v_{\parallel} + \text{irrelevant terms} \quad (4)$$

In the steady state, we can solve the right hand side of Eq. 4 and get the following solution for v_{\parallel}

$$v_{\parallel} = -D_2 \partial_{\parallel} \delta \rho \quad (5)$$

where, $D_2 = \sigma_1/2\alpha$. Inserting Eq.5 in the linearised equations of motion for v_{\perp} and $\delta \rho$ and neglecting the irrelevant terms,

$$\partial_t v_{\perp} + \gamma \partial_{\parallel} v_{\perp} = -\sigma_1 \partial_{\perp} \delta \rho + D_T \nabla^2 v_{\perp} + f_{\perp} \quad (6)$$

and density equation in Eq.1(main text),

$$\partial_t \delta \rho + v_0 \partial_{\parallel} \delta \rho - D_2 \rho_0 \partial_{\parallel}^2 \delta \rho - D_{\rho} \nabla^2 \delta \rho + \rho_0 \partial_{\perp} v_{\perp} = -\lambda \rho_0 \delta \rho \quad (7)$$

where D_2, D_{ρ}, D_B and D_T are the diffusion constants, $\gamma = \lambda_1 v_0$. For the given system parameters, they are all constants. To further study the solution of above linearised equations we define a vector $\mathbf{A}(\mathbf{r}, t) = (v_{\perp}, \delta \rho)$. Eq. 6 and Eq.7, we write the equations in Fourier space by defining

$$\mathbf{A}(\mathbf{r}, t) \simeq \int \mathbf{A}(\mathbf{q}, \omega) \exp(-i\omega t + i\mathbf{q} \cdot \mathbf{r}) d\mathbf{q} d\omega$$

Now we can write the linear equations for $v_{\perp}(\mathbf{q}, \omega)$ and $\delta \rho(\mathbf{q}, \omega)$

$$[-i(\omega - \gamma q_{\parallel}) + \Gamma_L] v_{\perp} + i\sigma_1 q_{\perp} \delta \rho = f_{\perp} \quad (8)$$

and

$$[-i(\omega - v_0 q_{\parallel}) + \Gamma_{\rho} + \lambda \rho_0] \delta \rho + i\rho_0 q_{\perp} v_{\perp} = 0 \quad (9)$$

where $\mathbf{q} = (q_{\parallel}, q_{\perp}) = q(\cos(\theta), \sin(\theta))$, where θ is the angle from the direction of broken symmetry. The Fourier transform of random force $f_{\perp}(\mathbf{q}, \omega)$ has properties $\langle f_{\perp}(\mathbf{q}, \omega) \rangle = 0$ and variance $\langle f_{\perp}(\mathbf{q}, \omega) f_{\perp}(\mathbf{q}', \omega') \rangle = \Delta \delta(\mathbf{q} + \mathbf{q}') \delta(\omega + \omega')$; The two damping $\Gamma_{L,\rho}(\mathbf{q})$ defined as $\Gamma_L(\mathbf{q}) = D_T(q_{\parallel}^2 + q_{\perp}^2)$ and $\Gamma_{\rho}(\mathbf{q}) = D_2 \rho_0 q_{\parallel}^2 + D_{\rho}(q_{\parallel}^2 + q_{\perp}^2)$. The linear equations Eq.8 and Eq.9 for v_{\perp} and $\delta \rho$ can be solved using following matrix;

$$\begin{bmatrix} -i(\omega - \gamma q_{\parallel}) + \Gamma_L & i\sigma_1 q_{\perp} \\ iq_{\perp} \rho_0 & -i(\omega - v_0 q_{\parallel}) + \Gamma_{\rho} + \lambda \rho_0 \end{bmatrix} \begin{bmatrix} v_{\perp} \\ \delta \rho \end{bmatrix} = \begin{bmatrix} f_L \\ 0 \end{bmatrix}$$

The solutions for v_{\perp} and $\delta \rho$ is

$$\begin{bmatrix} v_{\perp} \\ \delta \rho \end{bmatrix} = [M]^{-1} \begin{bmatrix} f_T \\ 0 \end{bmatrix}$$

where the matrix $[M]$ is,

$$[M] = \begin{bmatrix} -i(\omega - \gamma q_{\parallel}) + \Gamma_L & i\sigma_1 q_{\perp} \\ iq_{\perp} \rho_0 & -i(\omega - v_0 q_{\parallel}) + \Gamma_{\rho} + \lambda \rho_0 \end{bmatrix}$$

and $[M]^{-1}$ is

$$[M^{-1}] = \frac{1}{\det[M]} \begin{bmatrix} -i(\omega - v_0 q_{\parallel}) + \Gamma_{\rho} + \lambda \rho_0 & -i\sigma_1 q_{\perp} \\ -iq_{\perp} \rho_0 & -i(\omega - \gamma q_{\parallel}) + \Gamma_L \end{bmatrix}$$

where

$$c_2(\theta_{\mathbf{q}}) = \sqrt{\frac{1}{4}(\gamma - v_0)^2 \cos^2(\theta_{\mathbf{q}}) + c_0^2 \sin^2(\theta_{\mathbf{q}})}$$

$$\begin{aligned} \det[M] &= -\omega^2 + \omega(v_0 q_{\parallel} + \gamma q_{\parallel} - i\Gamma_{\rho} - i\Gamma_L - i\lambda \rho_0) \\ &\quad - v_0 \gamma q_{\parallel}^2 + iq_{\parallel}(\gamma \Gamma_{\rho} + v_0 \Gamma_L) + \Gamma_{\rho} \Gamma_L \\ &\quad + \rho_0 \sigma_1 q_{\perp}^2 + \Gamma_L \lambda \rho_0 + i\lambda \rho_0 \gamma q_{\parallel} \end{aligned}$$

(10)

$$c_0 = \sqrt{\sigma_1 \rho_0}$$

and $\Delta \Gamma = \widehat{\Gamma}_{\rho} - \widehat{\Gamma}_L$, $\widehat{\Gamma}_L = D_T$, $\widehat{\Gamma}_{\rho} = D_2 \rho_0 \cos \theta + D_{\rho}$. We can calculate the speed of sound wave $C(q, \lambda, \theta) = \frac{d\omega_{\pm}}{dq}$ from Eq. 12 as

$$C(q, \lambda, \theta) = \frac{\gamma + v_0}{2} \cos(\theta_{\mathbf{q}})$$

The quadratic equation for the ω ;

$$\begin{aligned} \omega^2 - \omega[q_{\parallel}(v_0 + \gamma) - i(\Gamma_{\rho} + \Gamma_L + \lambda \rho_0)] \\ - iq_{\parallel}(\gamma \Gamma_{\rho} + v_0 \Gamma_L) + v_0 \gamma q_{\parallel}^2 \\ - \rho_0 \sigma_1 q_{\perp}^2 - \Gamma_L \lambda \rho_0 - i\lambda \rho_0 \gamma q_{\parallel} = 0 \end{aligned}$$

(11)

$$\begin{aligned} &+ \sqrt{\frac{1}{4}(\gamma - v_0)^2 \cos^2(\theta_{\mathbf{q}}) + c_0^2 \sin^2(\theta_{\mathbf{q}})} \\ &\quad - \frac{\Delta \Gamma \lambda \rho_0}{\sqrt{\frac{1}{4}(\gamma - v_0)^2 \cos^2(\theta_{\mathbf{q}}) + c_0^2 \sin^2(\theta_{\mathbf{q}})}} \\ &\quad + \frac{(\lambda \rho_0)^2}{q^2 \sqrt{\frac{1}{4}(\gamma - v_0)^2 \cos^2(\theta_{\mathbf{q}}) + c_0^2 \sin^2(\theta_{\mathbf{q}})}} \end{aligned}$$

(13)

The real part two solutions of ω_{\pm} are given by;

$$\begin{aligned} \omega_{\pm} &= c_{\pm}(\theta_{\mathbf{q}})q - \frac{\Delta \Gamma \lambda \rho_0 q}{\sqrt{(\frac{\gamma - v_0}{2})^2 \cos^2 \theta + c_0^2 \sin^2 \theta}} \\ &\quad - \frac{(\lambda \rho_0)^2}{2q \sqrt{(\frac{\gamma - v_0}{2})^2 \cos^2 \theta + c_0^2 \sin^2 \theta}} \end{aligned}$$

(12)

For the case $\theta = 0$, the speed of sound wave from Eq.12 as

$$C(q, \lambda) = \frac{d\omega_{\pm}}{dq} = v_0 - \frac{2\Delta \Gamma \lambda \rho_0}{(\gamma - v_0)} + \frac{4(\lambda \rho_0)^2}{q^2(\gamma - v_0)^2}$$

(14)

Further we go back to the solution for v_{\perp} and $\delta \rho$

$$v_{\perp}(\mathbf{q}, \omega) = G_{LL}(\mathbf{q}, \omega) f_{\perp}(\mathbf{q}, \omega)$$

(15)

$$\delta \rho(\mathbf{q}, \omega) = G_{\rho L}(\mathbf{q}, \omega) f_{\perp}(\mathbf{q}, \omega)$$

(16)

where the propagators G_{LL} and $G_{\rho L}$ are given by;

$$G_{LL}(\mathbf{q}, \omega) = \frac{(-i(\omega - v_0 q_{\parallel}) + \Gamma_{\rho}(\mathbf{q}) + \lambda \rho_0)}{(\omega - c_{+}(\theta_{\mathbf{q}})q)(\omega - c_{-}(\theta_{\mathbf{q}})q) + i\omega(\Gamma_L(\mathbf{q}) + \Gamma_{\rho}(\mathbf{q}) + \lambda \rho_0) - iq \cos \theta (\gamma \Gamma_L(\mathbf{q}) + v_0 \Gamma_{\rho}(\mathbf{q}) + 2\lambda \rho_0 (\gamma + v_0))}$$

(17)

$$G_{\rho L}(\mathbf{q}, \omega) = \frac{-i\sigma_1 q_{\perp}}{(\omega - c_+(\theta_{\mathbf{q}})q)(\omega - c_-(\theta_{\mathbf{q}})q) + i\omega(\Gamma_L(\mathbf{q}) + \Gamma_{\rho}(\mathbf{q}) + \lambda\rho_0) - iq \cos\theta(\gamma\Gamma_L(\mathbf{q}) + v_0\Gamma_{\rho}(\mathbf{q}) + 2\lambda\rho_0(\gamma + v_0))} \quad (18)$$

Hence, the two-point density-density correlation function $C_{\rho}(\mathbf{q}, \omega)$ will become;

$$C_{\rho}(q, \omega) = \frac{\Delta\rho_0^2 q_{\perp}^2}{(\omega - c_+(\theta_{\mathbf{q}})q)^2(\omega - c_-(\theta_{\mathbf{q}})q)^2 + (\omega(\Gamma_L(\mathbf{q}) + \Gamma_{\rho}(\mathbf{q}) + \lambda\rho_0) - q \cos\theta(\gamma\Gamma_L(\mathbf{q}) + v_0\Gamma_{\rho}(\mathbf{q}) + 2\lambda\rho_0(\gamma + v_0)))^2} \quad (19)$$

The C_{ρ} has two sharp peaks at $\omega = c_{\pm}q$ with width $\mathcal{O}(q^2)$. The width of these peaks in the limit $q \rightarrow 0$, is very small compared to its displacement from the origin ($\mathcal{O}(\omega)$). The expression for the structure factor $S(q) = C_{\rho}(q) = \int_{-\infty}^{+\infty} C_{\rho}(\mathbf{q}, \omega) \frac{d\omega}{2\pi}$ is

$$S(q) = \frac{\Delta_0 \rho_0^2 q_{\perp}^2 + c_{\pm}^2 q^2 \lambda^2 \rho_0^2}{[c_{\pm} q(\Gamma_L(\mathbf{q}) + \Gamma_{\rho}(\mathbf{q}) + \lambda\rho_0)]^2} \times \left[1 + \frac{\Gamma_{\rho}(\mathbf{q})}{\Gamma_L(\mathbf{q})} + \frac{2\lambda\rho_0(\gamma + v_0 + 0.5)}{\Gamma_L(\mathbf{q})} \right] \quad (20)$$

Here we have neglected the higher order term of $\mathcal{O}(q^4)$. We write the expression for small λ such that we can

ignore the term of order $\mathcal{O}(\lambda^2)$. Writing the different values of constants from the numerical simulation we get,

$$S(q) = \frac{A[q^2 + B\lambda]}{[Cq^2 + D\lambda]^2}$$

where $A = 0.056$, $B = 2.25$, $C = 0.86$, $D = 0.75$. We can now calculate the number fluctuation ΔN in a volume V as $\sqrt{S(q \rightarrow 0)V}$. We get the expression for ΔN as

$$\Delta N = N \frac{\sqrt{A(1 + BN\lambda)}}{C + DN\lambda} \quad (21)$$

-
- [1] S. Ramaswamy, Annu. Rev. Condens. Matter Phys. **1**, 323 (2010).
- [2] M. C. Marchetti, J.-F. Joanny, S. Ramaswamy, T. B. Liverpool, J. Prost, M. Rao, and R. A. Simha, Reviews of modern physics **85**, 1143 (2013).
- [3] J. Toner, Y. Tu, and S. Ramaswamy, Annals of Physics **318**, 170 (2005).
- [4] C. Bechinger, R. Di Leonardo, H. Löwen, C. Reichhardt, G. Volpe, and G. Volpe, Reviews of Modern Physics **88**, 045006 (2016).
- [5] T. Vicsek, A. Czirók, E. Ben-Jacob, I. Cohen, and O. Shochet, Physical review letters **75**, 1226 (1995).
- [6] V. Semwal, S. Dikshit, and S. Mishra, The European Physical Journal E **44**, 1 (2021).
- [7] F. Cichos, K. Gustavsson, B. Mehlig, and G. Volpe, Nature Machine Intelligence **2**, 94 (2020).
- [8] D. Needleman and Z. Dogic, Nature reviews materials **2**, 1 (2017).
- [9] G. De Magistris and D. Marenduzzo, Physica A: Statistical Mechanics and its Applications **418**, 65 (2015).
- [10] É. Fodor and M. C. Marchetti, Physica A: Statistical Mechanics and its Applications **504**, 106 (2018).
- [11] L. Balasubramaniam, R.-M. Mège, and B. Ladoux, Current Opinion in Genetics & Development **73**, 101897 (2022).
- [12] T. Feder, Physics today **60**, 28 (2007).
- [13] A. Bottinelli, D. Sumpter, and J. Silverberg, in *APS March Meeting Abstracts*, Vol. 2017 (2017) pp. H14–004.
- [14] B. Liebchen and D. Levis, Physical review letters **119**, 058002 (2017).
- [15] B. Mahault, X.-c. Jiang, E. Bertin, Y.-q. Ma, A. Patelli, X.-q. Shi, and H. Chaté, Physical review letters **120**, 258002 (2018).
- [16] B. Bhattacharjee, S. Mishra, and S. Manna, Physical Review E **92**, 062134 (2015).
- [17] H. Chaté, F. Ginelli, G. Grégoire, and F. Raynaud, Physical Review E **77**, 046113 (2008).
- [18] S. Mishra and S. Pattanayak, Physica A: Statistical Mechanics and its Applications **477**, 128 (2017).
- [19] J. P. Singh, S. Pattanayak, and S. Mishra, Journal of Physics A: Mathematical and Theoretical **54**, 115001 (2021).
- [20] S. Dikshit and S. Mishra, The European Physical Journal E **45**, 1 (2022).
- [21] T. B. Liverpool, Physical Review E **67**, 031909 (2003).
- [22] N. D. Mermin and H. Wagner, Physical Review Letters **17**, 1133 (1966).
- [23] Y. Tu, J. Toner, and M. Ulm, Physical review letters **80**, 4819 (1998).
- [24] J. Toner and Y. Tu, Physical review letters **75**, 4326 (1995).
- [25] J. Toner and Y. Tu, Physical review E **58**, 4828 (1998).
- [26] T. Vicsek, A. Czirók, E. Ben-Jacob, I. Cohen, and O. Shochet, Physical review letters **75**, 1226 (1995).
- [27] J. Toner, Physical review letters **108**, 088102 (2012).
- [28] T. R. Malthus, D. Winch, and P. James, *Malthus: 'An Essay on the Principle of Population'* (Cambridge University Press, 1992).
- [29] A. J. Bray, Advances in Physics **51**, 481 (2002).
- [30] T. R. Malthus and T. Malthus, *An essay on the principle of population* (Routledge/Thoemmes Press London, 1996).
- [31] P. K. Mishra and S. Mishra, Physics of Fluids **34**, 057110 (2022), <https://doi.org/10.1063/5.0086952>.
- [32] N. Goldenfeld, *Lectures on phase transitions and the renormalization group* (CRC Press, 2018).
- [33] V. Bally and D. Talay, Probability theory and related fields **104**, 43 (1996).

- [34] P. C. Hohenberg and B. I. Halperin, *Reviews of Modern Physics* **49**, 435 (1977).
- [35] R. Das, S. Mishra, and S. Puri, *EPL (Europhysics Letters)* **121**, 37002 (2018).
- [36] I. M. Lifshitz and V. V. Slyozov, *Journal of physics and chemistry of solids* **19**, 35 (1961).
- [37] S. Mishra, A. Baskaran, and M. C. Marchetti, *Physical Review E* **81**, 061916 (2010).
- [38] P. M. Chaikin, T. C. Lubensky, and T. A. Witten, *Principles of condensed matter physics*, Vol. 10 (Cambridge university press Cambridge, 1995).
- [39] R. Voituriez, J.-F. Joanny, and J. Prost, *EPL (Europhysics Letters)* **70**, 404 (2005).
- [40] K. Kruse, J.-F. Joanny, F. Jülicher, J. Prost, and K. Sekimoto, *The European Physical Journal E* **16**, 5 (2005).
- [41] W. Mather, O. Mondragón-Palomino, T. Danino, J. Hasty, and L. S. Tsimring, *Physical review letters* **104**, 208101 (2010).
- [42] D. Karig, K. M. Martini, T. Lu, N. A. DeLateur, N. Goldenfeld, and R. Weiss, *Proceedings of the National Academy of Sciences* **115**, 6572 (2018).
- [43] M. E. Cates, D. Marenduzzo, I. Pagonabarraga, and J. Tailleur, *Proceedings of the National Academy of Sciences* **107**, 11715 (2010).
- [44] D. Dell’Arciprete, M. Blow, A. Brown, F. Farrell, J. S. Lintuvuori, A. McVey, D. Marenduzzo, and W. C. Poon, *Nature communications* **9**, 1 (2018).